MURA 543

Reprinted from
Proceedings of the Intern. Conf.
on High-Energy Accelerators and
Instrumentation - CERN 1959

Fermilab Library
0 1160 0038829 2

THE MURA TWO-WAY ELECTRON ACCELERATOR

by the MURA staff

Midwestern Universities Research Association, Madison, Wis. (*)

(presented by K. R. Symon)

I. INTRODUCTION

A two-beam Ohkawa radial sector FFAG accelerator[1] which will accelerate electrons to approximately 40 MeV is being constructed by MURA. Preliminary planning was begun in the summer of 1957, as construction of the MURA spiral sector electron accelerator[2] was being completed. The primary goal was fixed as the production and study of large accelerated currents and beam handling methods with these currents. It was also considered desirable to gain experience with higher magnetic field strengths than those in the earlier MURA accelerators[2, 3].

TABLE I

Parameters of the MURA two-way electron accelerator

N (Number of sectors)	16	Magnet weight :	
k (mean field index)	9.3	Fe	32 tons
ν_x	6.36	Cu	7 tons
ν_y	5.34	Magnet power	120 kW
C (circumference factor)	8.04	Peak RF power at 500 V peak	3.5 kW
Orbit crossing angle	49°		
Orbit scalloping	$\pm 0.027r$		

	Injection orbit	Transition	Final orbit
Kinetic energy	100 keV	1.129 MeV	37.4 MeV
Average orbit sections	124.3 cm	151.6 cm	198 cm
Frequency of revolution	20.03 Mc/s	29.91 Mc/s	23.09 Mc/s
Maximum magnetic field	80 gauss		5000 gauss
Vertical aperture	5.6 cm		3.5 cm

By building a two-beam accelerator, it would also be possible to perform colliding-beam experiments.

The particles accelerated were chosen to be electrons to keep the radius and cost small. A time of the order of seconds is required to stack a large beam, which fixes the minimum final energy at about 30 MeV. For lower energies, the lifetime against gas scattering is smaller than 1 second. For electron-electron scattering experiments a much higher final energy (of order 200 MeV) would be desirable, in order to test quantum electrodynamics to smaller distances, but it was felt that such an accelerator would require more space and time than seemed expedient. Table I shows the main parameters of the accelerator.

II. ORBIT DESIGN STUDIES

The positive and negative field magnets are of equal length. When they are equally energized, beams can be accelerated in both directions simultaneously. When the negative field is lowered relative to the positive field, the circumference factor is decreased and one beam can be accelerated to a higher energy. The strength of the vertical focusing is decreased, which places a limit on the maximum final energy attainable.

The median plane magnetic field can be written in the form

$$B_r = B_\theta = 0$$

$$B_z = B_0 \left(\frac{r}{r_0}\right)^k \sum_{n=0}^{\infty} g_n \cos nN\theta \,, \qquad (1)$$

(*) Supported by the United States Atomic Energy Commission.

where r_0 is an arbitrary reference radius and N the number of sectors per revolution. The accelerator is *scaling*; i.e. the relative gradient k and the Fourier coefficients g_n are independent of radius. This insures that ν_x and ν_y, the numbers of radial and vertical betatron oscillations per revolution, are independent of radius (and thus of energy). At the two-way operating point, $g_n \neq 0$ only for n odd.

It is desirable that k be as large as possible in order to reduce the radial aperture and frequency modulation range necessary for a given momentum range. According to the smooth approximation results, ν_x varies as $k^{1/2}$ and we must have $\nu_x < \frac{1}{2} N$ to keep the radial motion within the first stability zone, so that k varies as N^2. But the straight section length available between magnets at a given radius decreases as N increases, so that there is a practical upper limit on k and N. It was felt that $N \leqslant 14$ would give values of k which were too small, while preliminary explorations showed that $N \simeq 20$ gave working points too close to the essential coupling resonance $\nu_x + 2\nu_y = N$. If one goes far enough above $N = 20$ to avoid this resonance, all the components become inconveniently small, as do the non-linear stability limits. $N = 16$ was chosen as affording a reasonable compromise among these factors.

The detailed orbit design was carried out using the MURA IBM-704 digital computer[4]. Magnetostatic problems can be solved with the " FOROCYL " program[3], and particle dynamics with the resulting fields can then be tested with the " FORMESH " program, for which several modifications are available for treating magnet error and misalignment effects.

There is no need to choose a unique one-way operating point, since any harmful resonance can be avoided by a different magnet excitation. The value of k was therefore chosen to give an optimum two-way operating point. The vertical aperture was chosen quite large in order to provide room for devices to be used in connection with particle handling experiments. As a result the field (Eq. (1)) is close to sinusoidal; for example, at the two-way operating point $g_3 \simeq 0.06\ g_1$ and all higher harmonics are considerably smaller. A magnet cross-section at fixed radius is shown in Fig. 1. The magnets are cut back above the poleface to provide a shelf for the poleface backwinding return currents, thus increasing the usable free space between magnets.

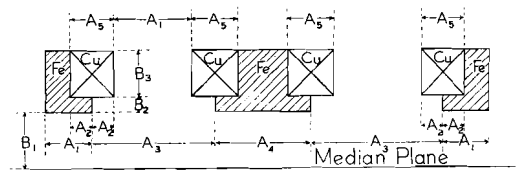

Fig. 1. Magnet pole cross-section at fixed radius in the scaling pole region.

Dimensions in units of radius:

$A_1 = 0.0549779$	$A_5 = 0.03141593$
$A_2 = 0.01570796$	$B_1 = 0.03926991$
$A_3 = 0.0863938$	$B_2 = 0.01570796$
$A_4 = 0.1099557$	$B_3 = 0.07068584$

Table II gives various parameters for the two-way operating point and two typical one-way points. For all of these points, $N = 16$, $k = 9.3$, the maximum orbit radius is 203 cm and the peak magnetic field is 5000 gauss.

TABLE II

Relative excitation (+/–)	Circumference factor	ν_x	ν_y	Final energy (MeV)
1	8.04	6.36	5.34	37.4
1.222	6.43	4.74	3.33	46.4
1.381	5.68	4.28	2.32	52.7

Misalignment effects were also investigated by digital computation. A detailed discussion is given elsewhere[4].

III. MAGNET DESIGN

The radial field variation k (see Eq. (1)) is produced in two different ways in different radial regions. From 110 cm to 190 cm, a scaling pole with backwound poleface currents is employed, while from 190 cm to 207 cm, the radial variation is produced by a " non-scaling " pole, a machined equipotential surface without poleface currents.

The scaling pole is similar in principle to those in the earlier MURA accelerators. All dimensions are proportional to radius. In the present design, the poleface windings are embedded in azimuthal slots rather than distributed in layers on the poleface. This was done to provide more usable vertical gap and to fix accurately the position of each winding. The

effects of this winding style on particle dynamics were investigated with the digital computer [5] and shown to be small for this particular design. Fig. 1 provides a view of the scaling pole region.

Fig. 2 shows the scaling pole with computed values of the magnetostatic equipotnetial surfaces generated by the poles. The same field can be generated by an equipotential surface which follows correctly these surfaces as a function of radius. In practice, simple approximations to such a surface which curve only in the radial direction give accurately the desired field. Clearly, the same surface is not correct for all relative magnet excitations. If one attempted to use a non-scaling pole machined correctly for the two-way operating point at the second one-way point of Table II, ν_x would change by about a half-integer across the non-scaling pole. Removable steel wedges at the sides of the non-scaling poles of the negative magnets are used to adjust the field properly as the

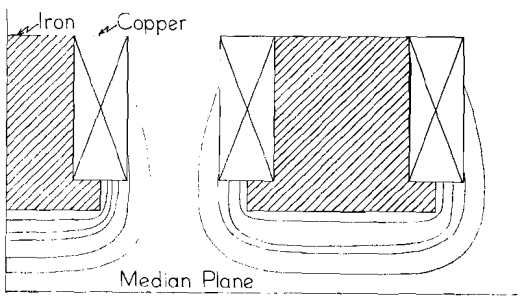

Fig. 2. Cross section of scaling pole with equipotential surfaces used to design the non-scaling pole.

excitation is changed. The design details are discussed elsewhere [4].

The magnets were machined by the Fairbanks-Morse Co., Beloit, Wisconsin from billets of a low carbon, aluminum-killed steel made for MURA by the Sharon Steel Co., Sharon, Pennsylvania. The magnet winding was done by the Northern Engineering Co., Baraboo, Wisconsin.

Fig. 3 is a photograph of one magnet showing the detail of the windings, slots and non-scaling pole. Fig. 4 shows the assembled magnets (without vacuum tank) during the field measurements.

IV. VACUUM TANK

The vacuum tank is constructed of welded 3/8″ aluminum sheets. It is strengthened by radial aluminum I-beams welded to the tank in the straight sections. The tank can be baked to 150° C by strip heaters mounted on the I-beams. The tank was constructed in four quadrants in the MURA shops. The two RF cavities are placed at quadrant junctions with machined Teflon sheet insulators sealed by " Viton-A " 0-rings.

Two different pumping systems have been tested, an oil diffusion pump system with cold-wall trapping and Varian Vacion pumps. Both gave satisfactory pressures, but the Vacion pumps were chosen because they are simpler and do not have deleterious effects on the vacuum system in the event of a power failure. Pressures of 2×10^{-8} mm Hg have been achieved in the separate quadrants.

It is planned that a second vacuum tank will be constructed of stainless steel with clearing electrodes to sweep out positive ions trapped by the stacked electron beams.

Fig. 5 shows the vacuum tank as it was assembled at the Fairbanks-Morse Co. for final flattening and rectifying of the flanges.

V. INJECTION SYSTEM

The source of electrons is a Machlett EG-300 X-ray tube with a hole drilled through the anode and redesigned envelope, giving 100 keV electrons. The beam is inflected into the accelerator by an electrostatic system which was designed by tracing particle orbits on the digital computer.

A programmed electrostatic field bump has been constructed to move the equilibrium orbit adiabatically away from the inflector during injection, so as to fill the betatron oscillation phase space more efficiently. This procedure was also designed by tracing particle orbits on the digital computer, the problem being complicated here by the presence of non-linear restoring forces. This computer work predicts that one should be able to inject about 20 turns.

It is planned to replace the X-ray tube with a more efficient source at some later time.

VI. ACCELERATION SYSTEM

For all operating points, the frequency of revolution is approximately 20 Mc/s at injection (100 keV), rises

to a maximum of about 30 Mc/s at transition energy, which occurs at 1.129 MeV kinetic energy, then falls to about 23 Mc/s at final energy. A betatron core is used to accelerate particles to 2 MeV, beyond the transition energy, where they are picked up by the RF system. The betatron core is split into four cores for convenience.

The RF system has two distinct parts, an accelerating system and a phase displacement system to make up for the energy lost by synchrotron radiation. Each part has a separate doubly-reentrant cavity with associated power amplifier, oscillator and control circuits. Both systems are broad-banded in order to provide more flexible frequency programming and to reduce beam cavity interaction. For example, the shunt impedance of the loaded acceleration cavity is about 36 ohm in the middle of the frequency range and it has a Q of about 3.6.

The accelerating system can accelerate 60 groups per second (in both directions) to provide large stacked current density, or 120 groups per second (in alternate directions), to provide large time-average current. In the two cases, the maximum voltages required are 250 and 500 V respectively [6].

The particles lose 19.4 MeV/s by synchrotron radiation, or about 1 eV per turn. Because of the energy width of the stacked beam, a large voltage would be required to hold the entire beam in stable synchrotron oscillations. In addition a certain amount of RF handling would be required to introduce each new pulse into the stacked beam. Hence we use a phase-displacement system to make up for the radiation loss. Empty buckets are moved down in energy through the stacked beam, moving it up in energy. The acceleration and phase-displacement systems operate simultaneously.

Fig. 6 is a photograph of one of the RF cavities.

VII. STATUS AND FUTURE PROGRAM

At the time of writing, construction of components is virtually completed and field measurements and corrections are expected to be completed in the near future. With the time needed for assembly, operation might be expected to begin about November 1, 1959. It is planned to concentrate first on accelerator experiments dealing with large stacked beams. A second injector system will be installed for future use in order to study colliding-beam experiments.

LIST OF REFERENCES

1. Ohkawa, T. Two-beam fixed field alternating gradient accelerator. Rev. sci. Instrum., *29*, p. 108-17, 1958.

2a. Kerst, D. W., Hausman, H. J., Haxby, R. O., Laslett, L. J., Mills, F. E., Ohkawa, T., Peterson, F. L., Sessler, A. M., Snyder, J. N. and Wallenmeyer, W. A. Operation of a spiral sector fixed field alternating gradient accelerator. Rev. sci. Instrum., *28*, p. 970-1, 1957.

b. Haxby, R. O., Laslett, L. J., Mills, F. E., Peterson, F. L., Rowe, E. M. and Wallenmeyer, W. A. Experience with a spiral sector FFAG electron accelerator. See p. 75.

3. Cole, F. T., Haxby, R. O., Jones, L. W., Pruett, C. H. and Terwilliger, K. M. Electron model fixed field alternating gradient accelerator. Rev. sci. Instrum., *28*, p. 403-20, 1957.

4. Cole, F. T. and Sessler, A. M. Design of a 50 MeV electron radial sector FFAG accelerator. MURA (*) 373. November 4, 1957.

5. Freiser, M. J. and Sessler, A. M. Effects of field bumps due to slotted poles. MURA (*) 366. October 21, 1957.

6. Johnston, L. H., Swenson, D. A. and Rowe, E. M. RF program for the 40 MeV two-way electron model. MURA (*) 426. August 22, 1958.

(*) See note on reports, p. 696.

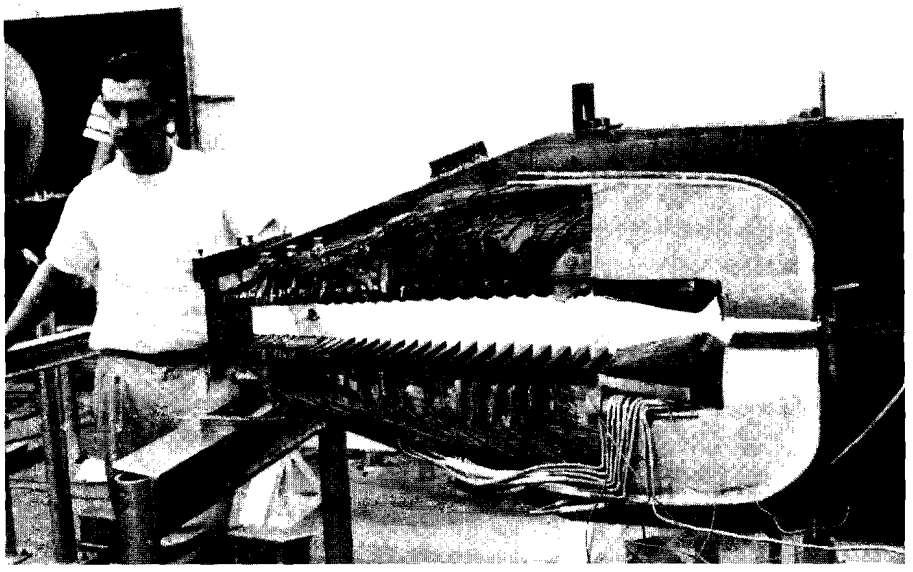

Fig. 3. A completed magnet pole, showing the windings, slots and non-scaling pole.

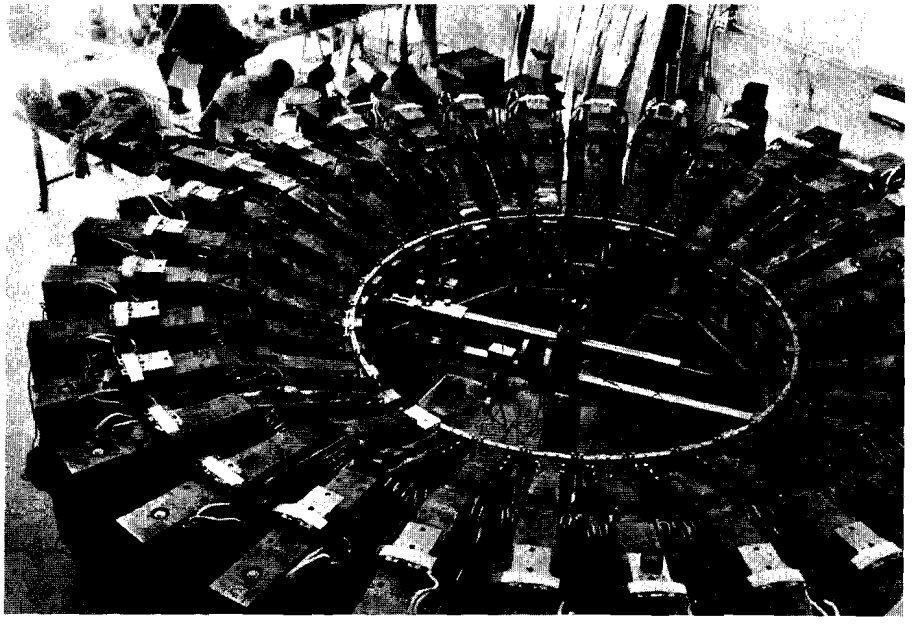

Fig. 4. Magnet assembly during field measurements.

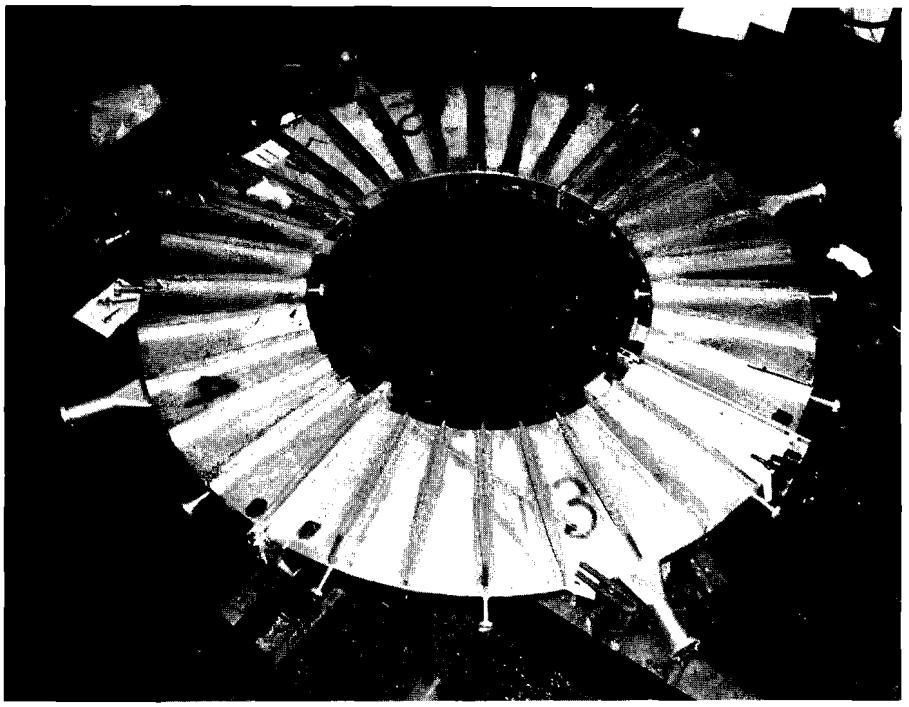

Fig. 5. The assembled vacuum tank, showing strengthening ribs, pumping and probe ports.

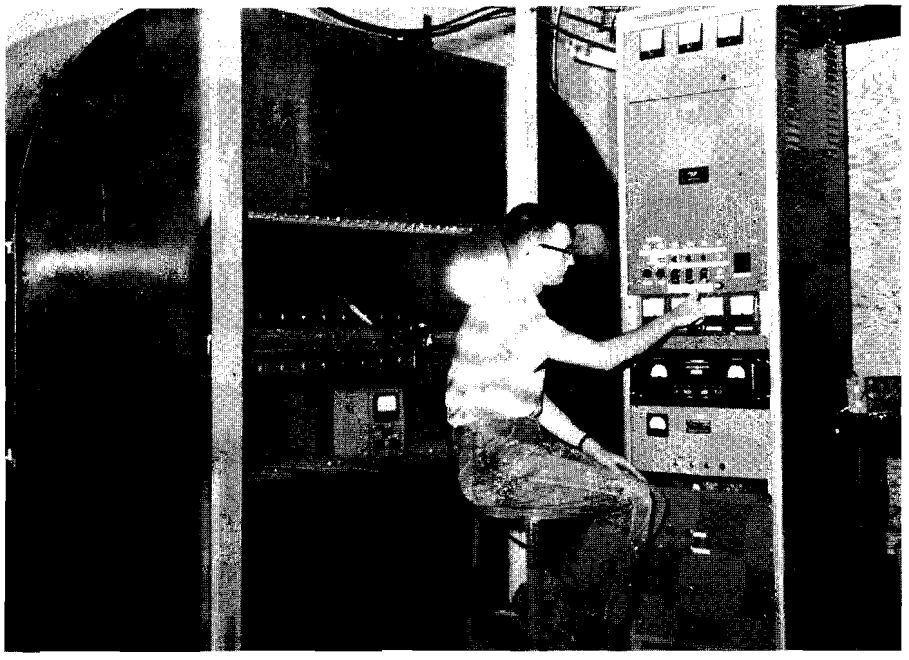

Fig. 6. An RF cavity.

MURA-543

THE MURA TWO-WAY ELECTRON ACCELERATOR

THE MURA STAFF

Midwestern Universities Research Association
Madison, Wisconsin (U.S.A.)*

*Supported by the United States Atomic Energy Commission.

I. Introduction

A two-beam Ohkawa radial sector FFAG accelerator[1)] which will accelerate electrons to approximately 40 Mev is being constructed by MURA. Preliminary planning was begun in the summer of 1957, as construction of the MURA spiral sector electron accelerator[2)] was being completed. The primary goal was fixed as the production and study of large accelerated currents and beam handling methods with these currents. It was also considered desirable to gain experience with higher magnetic field strengths than those in the earlier MURA accelerators[2), 3)]. By building a two-beam accelerator, it would also be possible to perform colliding beam experiments.

The particles accelerated were chosen to be electrons to keep the radius and cost small. A time of the order of seconds is required to stack a large beam, which fixes the minimum final energy at about 30 Mev. For lower energies, the lifetime against gas scattering is smaller than 1 second. For electron-electron scattering experiments a much higher final energy (of order 200 Mev) would be desirable, in order to test quan-

tum electrodynamics to smaller distances, but it was felt that such an accelerator would require more space and time than seemed expedient.

II. Orbit Design Studies

The positive and negative field magnets are of equal length. When they are equally energized, beams can be accelerated in both directions simultaneously. When the negative field is lowered relative to the positive field, the circumference factor is decreased and one beam can be accelerated to a higher energy. The strength of the vertical focusing is decreased, which places a limit on the maximum final energy attainable.

The median plane magnetic field can be written in the form

$$B_r = B_\theta = 0$$

$$B_z = B_o\left(\frac{r}{r_o}\right)^k \sum_{n=0}^{\infty} g_n \cos nN\theta \ , \tag{1}$$

where r_o is an arbitrary reference radius. The accelerator is <u>scaling</u>; i.e., the relative gradient k and the Fourier coefficients g_n are independent of radius. This insures that ν_x and ν_y, the numbers of radial and vertical betatron oscillations per revolution, are independent of radius (and thus of energy). At the two-way operating point, $g_n \neq 0$ only for n odd.

It is desirable that k be as large as possible in order to reduce the radial aperture and frequency swing necessary for a given momentum range. According to the smooth approximation results, ν_x varies as $k^{1/2}$ and we must have $\nu_x < \frac{1}{2}N$ to keep the radial motion within the first stability zone, so that k varies as N^2. But the straight section

length available between magnets at a given radius decreases as N increases, so that there is a practical upper limit on k and N. It was felt that $N \leq 14$ would give values of k which were too small, while preliminary explorations showed that $N \cong 20$ gave working points too close to the essential coupling resonance $\nu_x + 2\nu_y = N$. If one goes far enough above $N = 20$ to avoid this resonance, all the components become inconveniently small, as do the non-linear stability limits. $N = 16$ was chosen as affording a reasonable compromise among these factors.

The detailed orbit design was carried out using the MURA IBM 704 digital computer[4]. Magnetostatic problems can be solved with the "FOROCYL" program described in reference 3, and particle dynamics with the resulting fields can then be tested with the FORMESH program, for which are available several modifications for treating magnet error and misalignment effects.

There is no need to choose a unique one-way operating point, since any harmful resonance can be avoided by a different magnet excitation. The value of k was therefore chosen to give an optimum two-way operating point. The vertical aperture was chosen quite large in order to provide room for devices to be used in connection with particle handling experiments. As a result the field (1) is close to sinusoidal; for example, at the two-way operating point $g_3 \cong 0.06\, g_1$ and all higher harmonics are considerably smaller. A magnet cross section at fixed radius is shown in Fig. 1. The magnets are cut back above the poleface to provide a shelf for the poleface backwinding return currents, thus increas-

ing the useable free space between magnets.

Table I gives various parameters for the two-way operating point and two typical one-way points. For all of these points, N = 16, k = 9.3, the maximum orbit radius is 203 cm. and the peak magnetic field is 5000 gausses.

TABLE I

Relative Excitation (+/-)	Circum-ference factor	ν_x	ν_y	Final Energy (Mev)
1	8.04	6.36	5.34	37.4
1.222	6.43	4.74	3.33	46.4
1.381	5.68	4.28	2.32	52.7

Misalignment effects were also investigated by digital computation. A detailed discussion is given in reference 4.

III. Magnet Design

The radial field variation (k) is produced in two different ways in different radial regions. From 110 cm. to 190 cm., a scaling pole with backwound poleface currents is employed, while from 190 cm. to 207 cm., the radial variation is produced by a "non-scaling" pole, a machined equipotential surface without poleface currents.

The scaling pole is similar in principle to those in the earlier MURA accelerators. All dimensions are proportional to radius. In the present design, the poleface windings are embedded in azimuthal slots rather than distributed in layers on the poleface. This was done to provide more use-

able vertical gap and to fix accurately the position of each winding. The effects of this winding style on particle dynamics were investigated with the digital computer[5] and shown to be small for this particular design. Fig. 1 provides a view of the scaling pole region.

Fig. 2 shows the scaling pole with computed values of the magnetostatic equipotential surfaces generated by the poles. The same field can be generated by an equipotential surface which follows correctly these surfaces as a function of radius. In practice, simple approximations to such a surface which curve only in the radial direction give accurately the desired field. Clearly, the same surface is not correct for all relative magnet excitations. If one attempted to use a non-scaling pole machined correctly for the two-way operating point at the second one-way point of Table I, ν_y would change by about a half-integer across the non-scaling pole. Removable steel wedges at the sides of the non-scaling poles of the negative magnets are used to adjust the field properly as the excitation is changed. The design details are discussed in reference 4.

The magnets were machined by the Fairbanks-Morse Co., Beloit, Wisconsin from billets of a low carbon, aluminum-killed steel made for MURA by the Sharon Steel Co., Sharon, Pennsylvania. The magnet winding was done by the Northern Engineering Co., Baraboo, Wisconsin.

Fig. 3 is a photograph of one magnet showing the detail of the windings, slots and non-scaling pole. Fig. 4 shows the assembled magnets (without vacuum tank) during the field measurements.

IV. Vacuum Tank

The vacuum tank is constructed of welded 3/8" aluminum sheets. It is strengthened by radial aluminum I-beams welded to the tank in the straight sections. The tank can be baked to 150° C by strip heaters mounted on the I-beams. The tank was constructed in four quadrants in the MURA shops. The two rf cavities are placed at quadrant junctions with machined Teflon sheet insulators sealed by "Viton-A" 0-rings.

Two different pumping systems have been tested, an oil diffusion pump system with cold-wall trapping and Varian Vacion pumps. Both gave satisfactory pressures, but the Vacion pumps were chosen because they are simpler and do not have deleterious effects on the vacuum system in the event of a power failure. Pressures of 2×10^{-8} mm. Hg. have been achieved in the separate quadrants.

It is planned that a second vacuum tank will be constructed of stainless steel with clearing electrodes to sweep out positive ions trapped by the stacked electron beams.

Fig. 5 shows the vacuum tank as it was assembled at the Fairbanks-Morse Co. for truing up the flanges.

V. Injection System

The source of electrons is a Machlett EG-300 x-ray tube with a hole drilled through the anode and redesigned envelope, giving 100 kev electrons. The beam is inflected into the accelerator by an electrostatic system which was designed by tracing particle orbits on the digital computer.

A programmed electrostatic field bump has been constructed to move the equilibrium orbit adiabatically away from the inflector during injection, so as to fill the betatron oscillation phase space more efficiently. It was also designed by tracing particle orbits on the digital computer, the problem being complicated here by the presence of non-linear restoring forces. This computer work predicts that one should be able to inject about 20 turns.

It is planned to replace the x-ray tube with a more efficient source at some later time.

VI. Acceleration System

For all operating points, the frequency of revolution is approximately 20 megacycles/sec. at injection (100 kev) rises to a maximum of about 30 Mc/sec. at transition energy, which occurs at 1.129 Mev kinetic energy, then falls to about 23 Mc/sec. at final energy. A betatron core is used to accelerate particles to 2 Mev, beyond the transition energy, where they are picked up by the rf system. The betatron core is split into four cores for convenience.

The rf system has two distinct parts, an accelerating system and a phase displacement system to make up for the energy lost by synchrotron radiation. Each part has a separate doubly-re-entrant cavity with associated power amplifier, oscillator and control circuits. Both systems are broad banded in order to provide more flexible frequency programming and to reduce beam cavity interaction. For example, the shunt impedance of the loaded acceleration cavity is about 36 ohms in

the middle of the frequency range and it has a Q of about 3.6.

The accelerating system can accelerate 60 groups per second (in both directions) to provide large stacked current density, or 120 groups per second (in alternate directions), to provide large time-average current. In the two cases, the maximum voltages required are 250 and 500 volts, respectively[6].

The particles lose 19.4 Mev/sec. by synchrotron radiation, or about 1 ev per turn. Because of the energy width of the stacked beam, a large voltage would be required to hold the entire beam in stable synchrotron oscillations. In addition a certain amount of rf gymnastics would be required to introduce each new pulse into the stacked beam. Hence we use a phase-displacement system to make up for the radiation loss. Empty buckets are moved down in energy through the stacked beam, moving it up in energy. The acceleration and phase-displacement systems operate simultaneously.

Fig. 6 is a photograph of one of the rf cavities.

VII. Status and Future Program

At the time of writing, construction of components is virtually completed and field measurements and corrections are expected to be completed in the near future. With the time needed for assembly, operation might be expected to begin about November 1. It is planned to concentrate first on accelerator experiments dealing with large stacked beams. A second injector system will be installed for future use in order to study colliding beam experiments.

LIST OF REFERENCES

1. T. Ohkawa, Rev. Sci. Instr. 29, 108 (1958).
2. D. W. Kerst et al, Rev. Sci. Instr. 28, 970 (1957) and R. O. Haxby et al, Proceedings of this Conference.
3. F. T. Cole et al, Rev. Sci. Instr. 28, 403 (1957).
4. For a detailed description, see F. T. Cole and A. M. Sessler, MURA Report No. 373 (unpublished). Midwestern Universities Research Association, Madison, 1957. Available on request.
5. M. J. Freiser and A. M. Sessler, MURA Report No. 366 (unpublished). Midwestern Universities Research Association, Madison, 1957. Available on request.
6. L. H. Johnston, D. A. Swenson and E. M. Rowe, MURA Report No. 426 (unpublished). Midwestern Universities Research Association, Madison, 1958. Available on request.

CAPTIONS FOR FIGURES

Fig. 1. Magnet pole cross section at fixed radius in the scaling pole region.

Fig. 2. Cross section of scaling pole with equipotential surfaces used to design the non-scaling pole.

Fig. 3. A completed magnet pole, showing the windings, slots and non-scaling pole.

Fig. 4. Magnet assembly during field measurements.

Fig. 5. The assembled vacuum tank, showing strengthening ribs, pumping and probe ports.

Fig. 6. An rf cavity.

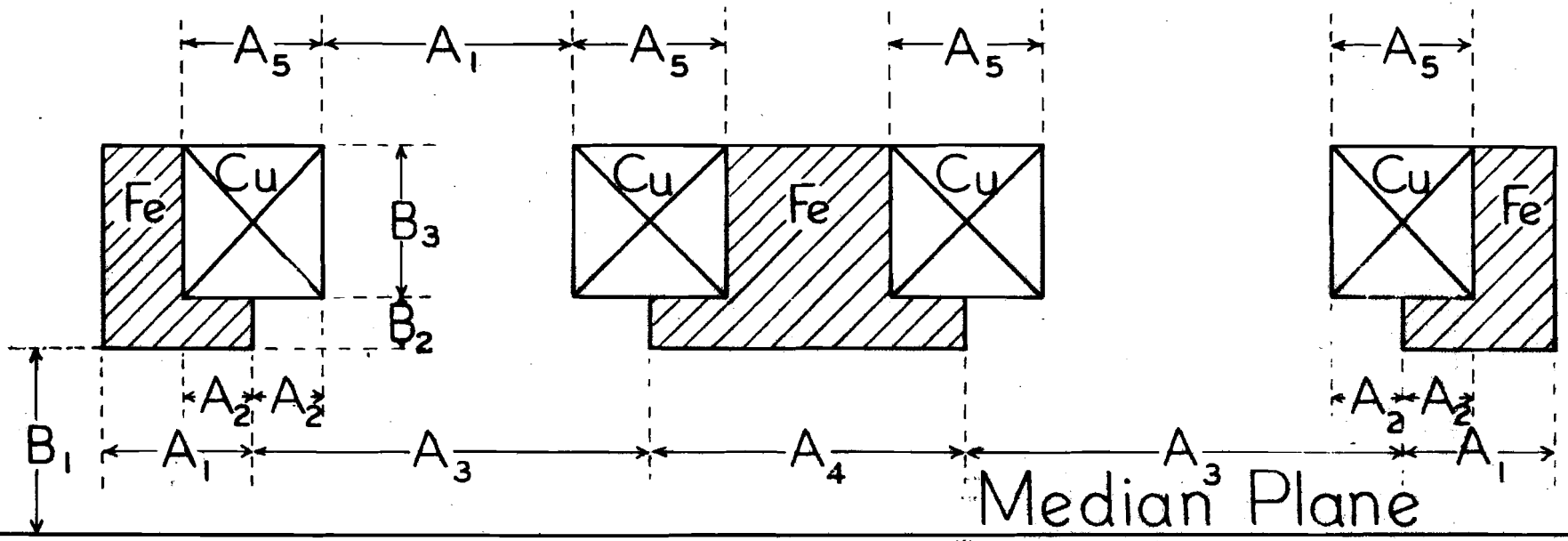

$A_1 = .0549779$

$A_2 = .01570796$

$A_3 = .0863938$

$A_4 = .1099557$

$A_5 = .03141593$

$B_1 = .03926991$

$B_2 = .01570796$

$B_3 = .07068584$

Dimensions in units of radius

Final Pole Geometry with Currents

Fig. I

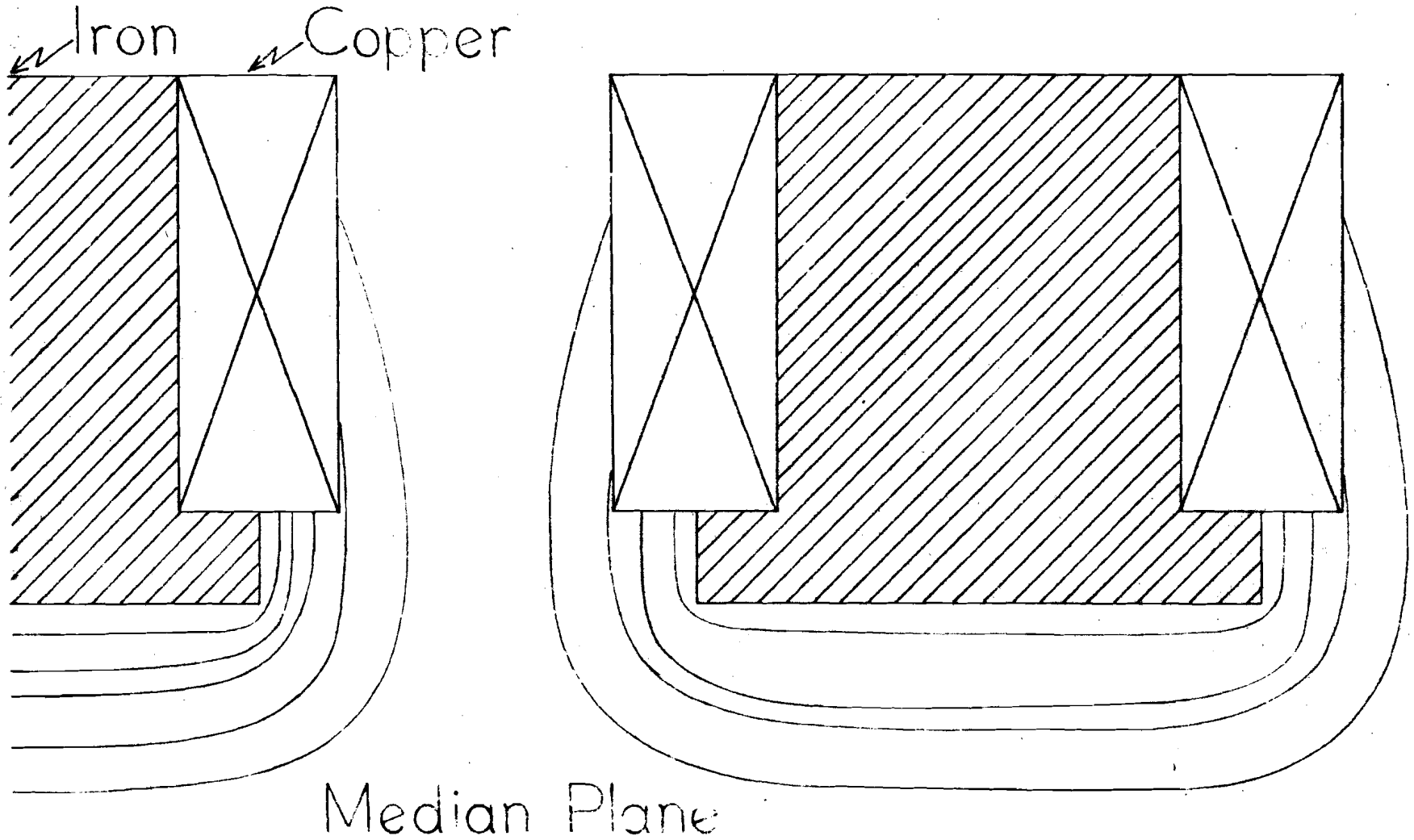

Magnetostatic Equipotentials for Two-Way Tuning

Fig. II

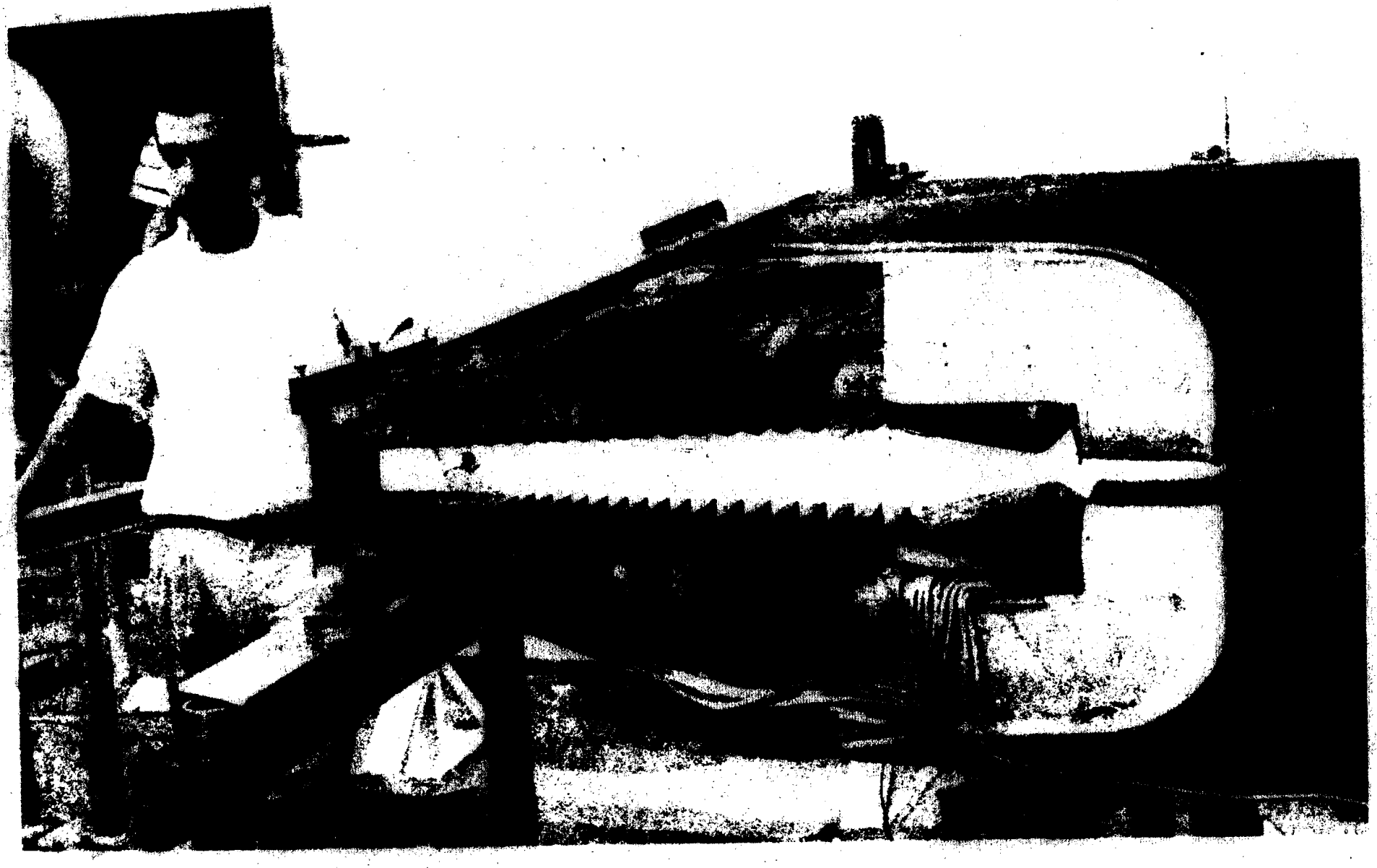

Fig 3

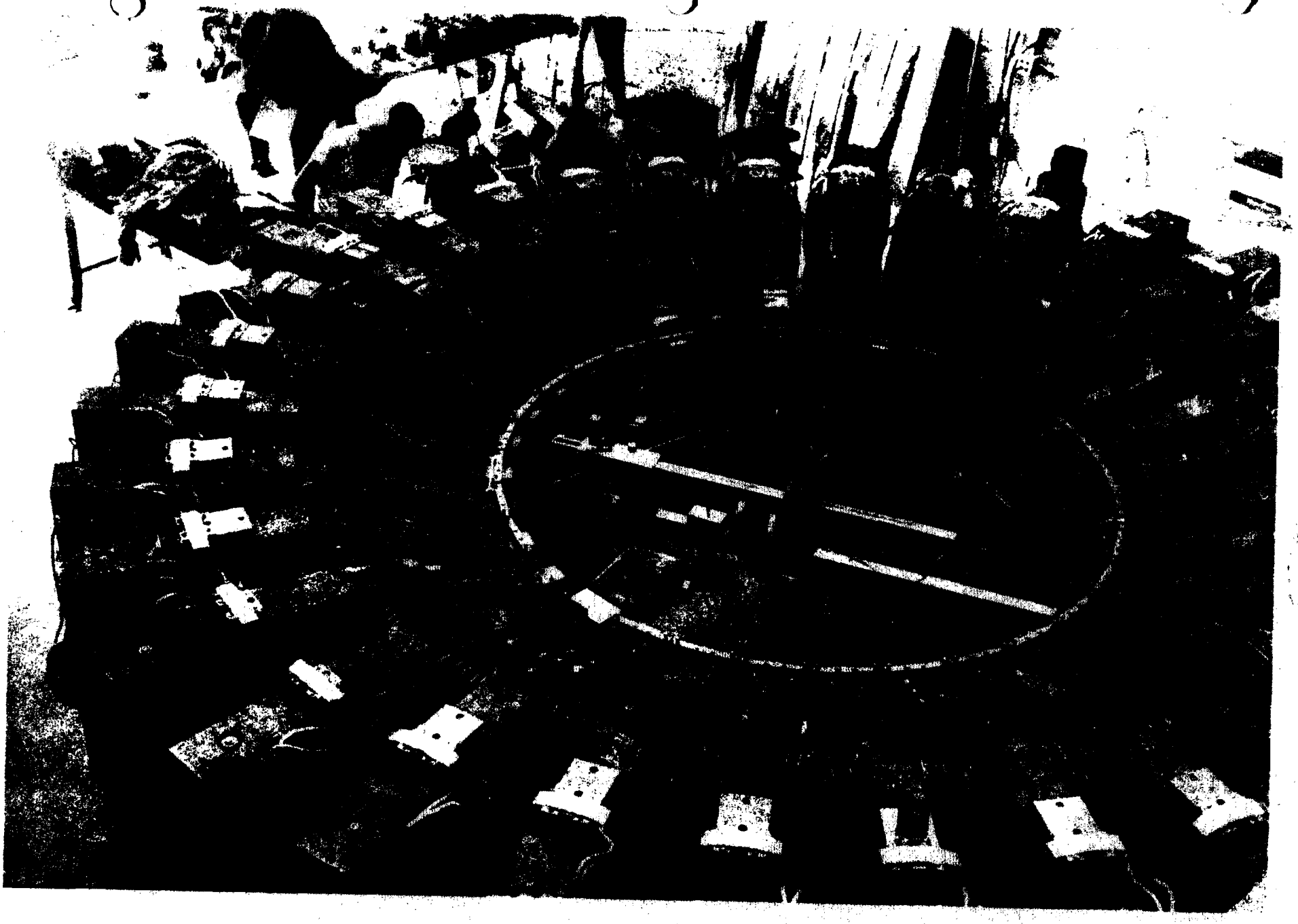

7194

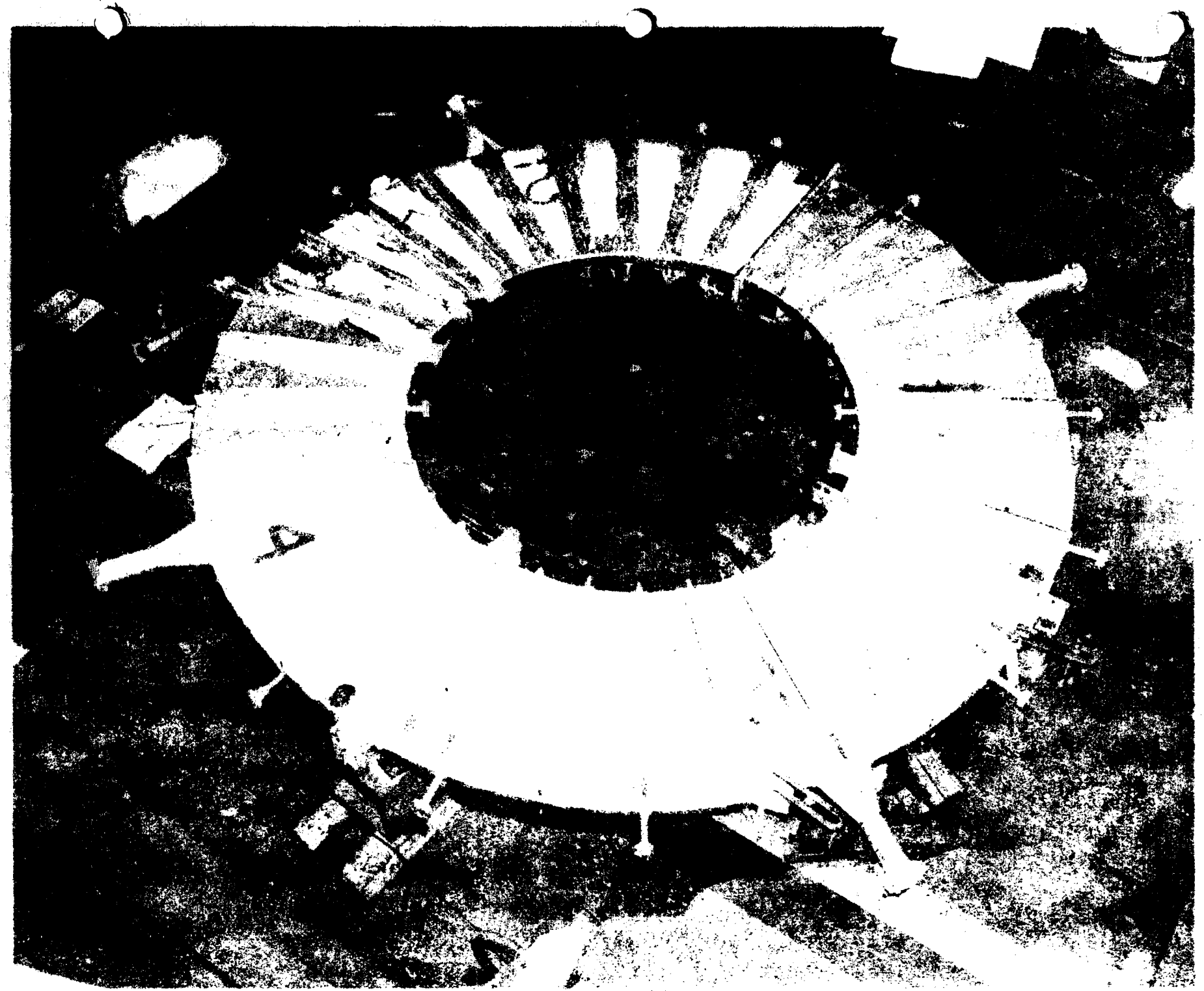

Fig 5